Journal of Magnetic Resonance 209 (2011) 156–160

Contents lists available at ScienceDirect

Journal of Magnetic Resonance

journal homepage: www.elsevier.com/locate/jmr

# Supercycled $SW_f$-TPPM sequence for heteronuclear dipolar decoupling in solid-state nuclear magnetic resonance

Cyril Augustine *, Narayanan D. Kurur

*Department of Chemistry, Indian Institute of Technology, New Delhi 110 016, India*

ARTICLE INFO

*Article history:*
Received 16 October 2010
Revised 29 December 2010
Available online 14 January 2011

*Keywords:*
Solid-state NMR
$^{13}C$–$^{1}H$ dipolar decoupling
Supercycled $SW_f$-TPPM
$SW_f$-TPPM
SPINAL-64

ABSTRACT

The performance of a supercycled $SW_f$-TPPM sequence for heteronuclear dipolar decoupling in solid-state NMR is analyzed here. The decoupling performance of this sequence with respect to experimental parameters, such as, the phase angle, proton offset and MAS frequency is studied. A comparison is made with two other commonly used decoupling schemes in solid-state NMR namely, SPINAL-64 and $SW_f$-TPPM, on a sample of U-$^{13}C$-labeled tyrosine. Our results show that supercycled $SW_f$-TPPM performs better than the former sequences. Also, numerical spin dynamics studies are presented which support the experimentally observed efficiency in the decoupling.



## 1. Introduction

Spectral resonances in solid-state NMR are usually broad due to the overlapping of strong interactions that depend on the orientation of nuclei in the magnetic field [1]. These interactions include homonuclear and heteronuclear dipole–dipole couplings, chemical shift anisotropy and electric quadrupolar couplings arising from the interaction of the non-spherical charge distribution of nuclei having spin $I > ½$ with the surrounding electric field gradient. However, heteronuclear dipolar decoupling gives significant improvement in the resolution of NMR spectra of solid samples. For instance, high-resolution solid-state NMR spectra of rare nuclei such as $^{13}C$ can be recorded with appropriate radio-frequency (RF) irradiation on the abundant $^{1}H$ spins along with magic angle spinning (MAS) to remove the dipolar couplings between $^{13}C$ and $^{1}H$ nuclei [1,2].

A continuous burst of RF irradiation on the most abundant spins during the acquisition of the signals from the rare nuclei, called continuous-wave (CW) decoupling was once considered as an effective technique for removing heteronuclear dipolar interactions in solids [1]. Two-pulse phase modulation (TPPM) [3] led to a most significant development in heteronuclear dipolar decoupling providing superior performance over the traditional CW decoupling. It was the first multi-pulse decoupling sequence in anisotropic systems. The TPPM sequence consists of repeating units of two RF pulses of equal length with alternating phases. It is of the form $\tau_{+\varphi}\ \tau_{-\varphi}$, where $\tau$ represents the pulse duration with a flip angle normally between 160° and 180° and $\varphi$ implies the phase angle around 15°. These two parameters $\tau$ and $\varphi$ are carefully optimized experimentally for superior performance.

After the invention of TPPM, a continuous quest for more effective decoupling sequences in anisotropic systems can be seen in the literature [6–21]. New sequences include small phase angle rapid cycling (SPARC) [6], small phase incremental alteration (SPINAL) [7], DROOPY sequences [8], XiX, a scheme with repeating units of two rotor-synchronized pulses with 180° phase shift [9], some symmetry based sequences [10,11], cosine modulated two-pulse phase modulation [12], decoupling schemes based on Hahn-Echo trains [13], sequences based on Swept-frequency two-pulse phase modulation [14–21] and Phase-Wiggled TPPM [22].

It has been proved in heteronuclear decoupling of isotropic liquids that the effectiveness of a decoupling sequence can be improved by combining different versions of the primitive cycle to form extended supercycles which results in the compensation of some of the residual pulse imperfections [4,5]. Later this idea was implemented in decoupling schemes for liquid crystals. For example, the SPARC-16 sequence was constructed by extending the basic TPPM scheme into a supercycle [6]. The SPARC-16, which stands for 'small phase angle rapid cycling with 16 steps', contains a step by step phase cycling of the parent TPPM decoupling sequence using 16 pulses. The incorporation of phase increments in the basic elements of TPPM led to the group of sequences called SPINAL which stands for small phase incremental alteration [7]. Among them SPINAL-64 works more effectively than TPPM for heteronuclear dipolar decoupling in anisotropic systems. In SPINAL-64 an extended supercycle is shaped from the basic element $Q = \tau$

* Corresponding author. Fax: +91 11 2658 1102.
*E-mail address:* cyril.augustinev@gmail.com (C. Augustine).

1090-7807/$ - see front matter © 2011 Elsevier Inc. All rights reserved.
doi:10.1016/j.jmr.2011.01.007

(10°) $\tau$ (−10°) $\tau$ (15°) $\tau$ (−15°) $\tau$ (20°) $\tau$ (−20°) $\tau$ (15°) $\tau$ (−15°), to formulate a decoupling scheme of $Q\ \overline{Q}\ \overline{Q}\ Q$ which contains 64 pulses. Here $\tau$ represents the pulse duration with a flip angle normally between 160° and 180° and $\overline{Q}$ is the phase inverted duplication of $Q$. For its effective performance the pulse flip angle is to be optimized. SPINAL-64 is one of the commonly used decoupling schemes for removing heteronuclear dipolar interactions in solids and static liquid crystals.

Swept-frequency TPPM ($SW_f$-TPPM), a recent decoupling sequence was formulated by modulating the pulse durations of TPPM blocks [14]. Here the phase modulation depth does not vary like SPINAL, but the pulse times ($\tau$) vary continuously during the sequence. There are 11 pulse pairs in the scheme and the pulse durations are varied in a pre-determined fashion from the beginning to the end. It is implemented by multiplying the pulse times ($\tau$) by a factor which varies from 0.78 to 1.22 so as to get a tangential sweep of the pulse length around the nominal $\pi$ pulse. The sequence $SW_f$-TPPM and some of its variants work admirably for heteronuclear dipolar decoupling in anisotropic systems [15,16]. It is experimentally demonstrated that these sequences can provide more effective decoupling band width when compared to TPPM and SPINAL-64 schemes which facilitated their application in liquid-crystal and solid-state NMR.

Recently, we have demonstrated that the supercycled version of $SW_f$-TPPM can be used effectively for removing heteronuclear dipolar interactions in liquid crystals [21]. The supercycled scheme was constructed in the form of $R\ R\ \overline{R}\ \overline{R}$, where $R$ is the parent $SW_f$-TPPM and $\overline{R}$ stands for the phase inverted counterpart of the parent sequence. It shows better decoupling characteristics than the other commonly used decoupling schemes in liquid-crystal NMR. In this article we analyze the performance of the supercycled $SW_f$-TPPM for heteronuclear dipolar decoupling in solid samples with respect to variation of three experimental parameters; the phase angle, proton offset, and the MAS frequency. Also, a systematic comparison is made with SPINAL-64 and the parent $SW_f$-TPPM. It is observed that supercycling increases the decoupling performance of $SW_f$-TPPM and the modified decoupling scheme is found to be more efficient than the former sequences with respect to the intensity enhancement observed in various decoupled spectral lines and the insensitivity of the resulting decoupling sequence towards proton offset and MAS frequency. Moreover the supercycled decoupling scheme is user-friendly and easy to apply on modern NMR spectrometers.

## 2. Experimental

A sample of U-$^{13}$C-labeled tyrosine (Sigma Chemical Company) was used for demonstrating the efficiencies of these decoupling schemes. All experiments were done on a Bruker AV spectrometer at a frequency of 500 MHz for proton equipped with a 4 mm triple resonance CPMAS probe at different MAS rates ranging from 6 to 14 kHz. For each experiment, eight scans were used to accumulate the $^{13}$C signals with a relaxation delay of 20 s. The $^{13}$C signals were enhanced by cross polarization (CP) with a contact time of 1 ms. Experiments were carried out at different decoupling field strengths such as 90, 75 and 55 kHz. The pulse durations and phase angles in each decoupling sequence were optimized using the intensity of decoupled $^{13}$C signal from the $CH_2$ carbon of glycine.

Numerical simulations were done to compare the efficiency of the parent $SW_f$-TPPM and its supercycled version for heteronuclear dipolar decoupling in solids using the SIMPSON program [23]. The selected spin system was a $^{13}$C nucleus dipolar-coupled to two protons. Both heteronuclear and homonuclear dipolar couplings were considered in the simulations and the calculations were done at different MAS frequencies (6, 8 and 14 kHz), phase angles (15–40°) and RF field strengths (80–160 kHz).

### 2.1. Design of decoupling schemes

SPINAL-64 is a supercycled decoupling scheme formulated by inclusion of phase increments in the basic elements of TPPM [7]. It is of the form $Q\ \overline{Q}\ \overline{Q}\ Q$. Here the basic element $Q$ is: 165(10°) 165(−10°) 165(15°) 165(−15°) 165(20°) 165(−20°) 165(15°) 165(−15°), and $\overline{Q}$ implies its phase inverted replica where, $\overline{Q}$ = 165(−10°) 165(10°) 165(−15°) 165(15°) 165(−20) 165(20°) 165(−15°) 165(15°). The optimized pulse flip angle is found to be around 165° and the initial phase angle is taken as 10°.

The $SW_f$-TPPM sequence [14] can be represented as, {[$0.78\tau_\varphi$ $0.78\tau_{-\varphi}$] [$0.86\tau_\varphi$ $0.86\tau_{-\varphi}$] [$0.94\tau_\varphi$ $0.94\tau_{-\varphi}$] [$0.96\tau_\varphi$ $0.96\tau_{-\varphi}$] [$0.98\tau_\varphi$ $0.98\tau_{-\varphi}$] [$\tau_\varphi$ $\tau_{-\varphi}$] [$1.02\tau_\varphi$ $1.02\tau_{-\varphi}$] [$1.04\tau_\varphi$ $1.04\tau_{-\varphi}$] [$1.06\tau_\varphi$ $1.06\tau_{-\varphi}$] [$1.14\tau_\varphi$ $1.14\tau_{-\varphi}$] [$1.22\tau_\varphi$ $1.22\tau_{-\varphi}$]}, where $\tau$ is a normal 180° pulse length $\varphi$ is the phase angle. Both $\tau$ and $\varphi$ are to be optimized for the better-quality performance of $SW_f$-TPPM.

A supercycled version of $SW_f$-TPPM was formulated from the parent sequence $R$. Here the supercycling was done in the form

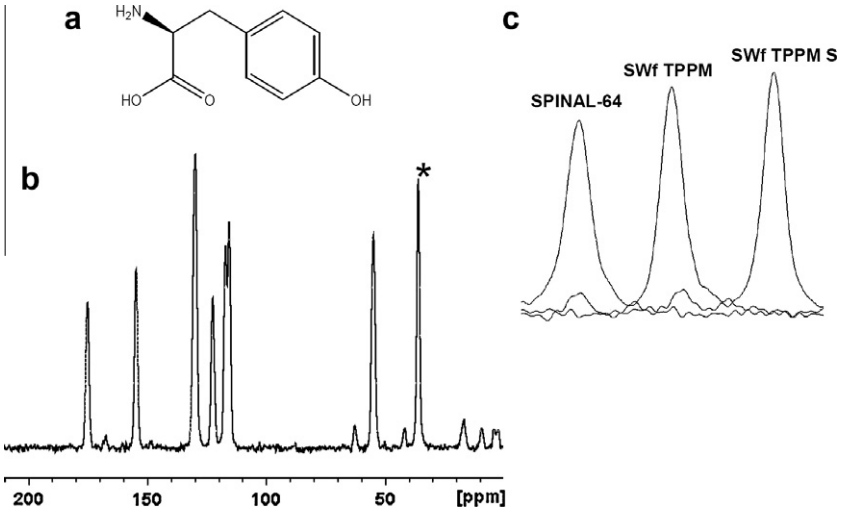


**Fig. 1.** (a) Chemical structure of tyrosine molecule, (b) $^{13}$C NMR spectrum of U-$^{13}$C-labeled tyrosine acquired with supercycled $SW_f$-TPPM decoupling. The decoupling power was 90 kHz with a MAS rate of 14 kHz. The $^{13}$C signal of $CH_2$ carbon is marked with asterisk. (c) The intensity comparison of the decoupled $^{13}$C signal of $CH_2$ carbon of the molecule using SPINAL-64, $SW_f$-TPPM and $SW_f$-TPPMS. Eight scans were used to acquire the $^{13}$C signals with a relaxation delay of 20 s for each experiment with a cross polarization (CP) contact time of 1 ms. The proton offset frequency is kept at 7.75 kHz which is far from the on-resonance position of the observed signal.

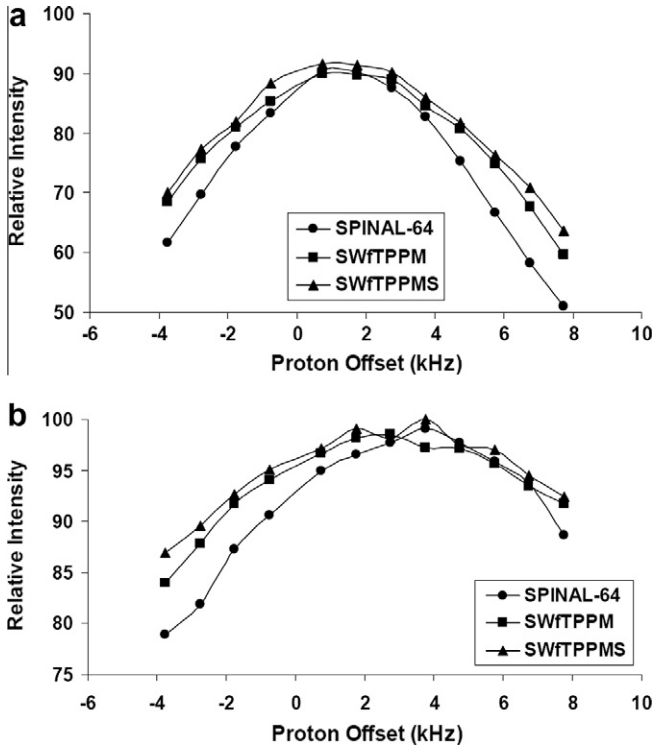


**Fig. 2.** The relative intensities of the (a) $CH_2$ (at 36 ppm) and (b) CH (130 ppm) carbons in the decoupled $^{13}C$ spectra of tyrosine recorded as a function of proton offset for SPINAL-64, $SW_f$-TPPM and $SW_f$-TPPMS decoupling. The RF power was 90 kHz with a MAS frequency of 14 kHz. In all cases the intensities are normalized with respect to the absolute intensity of the decoupled $^{13}C$ carbon of CH (130 ppm) recorded with $SW_f$-TPPMS with an RF power of 90 kHz at a proton offset of 3.75 kHz.

of $R\,R\,\overline{R}\,\overline{R}$, where $\overline{R}$ represents the phase inverted counterpart of the parent sequence, $\overline{R} = \{[0.78\tau_{-\phi}\,0.78\tau_{\phi}][0.86\tau_{-\phi}\,0.86\tau_{\phi}][0.94\tau_{-\phi}\,0.94\tau_{\phi}]\,[0.96\tau_{-\phi}\,0.96\tau_{\phi}][0.98\tau_{-\phi}\,0.98\tau_{\phi}]\,[\tau_{-\phi}\,\tau_{\phi}]\,[1.02\tau_{-\phi}\,1.02\tau_{\phi}]\,[1.04\tau_{-\phi}\,1.04\tau_{\phi}][1.06\tau_{-\phi}\,1.06\quad\tau_{\phi}][1.14\tau_{-\phi}\,1.14\tau_{\phi}][1.22\tau_{-\phi}\,1.22\tau_{\phi}]\}$. We denote this sequence as $SW_f$-TPPMS.

## 3. Results and discussion

The supercycled version of $SW_f$-TPPM is applied here in a standard sample of U-$^{13}C$-labeled tyrosine for heteronuclear dipolar decoupling between $^{13}C$ and $^{1}H$ and its efficiency of decoupling is compared with the other commonly used decoupling sequences in solids such as SPINAL-64 and the parent $SW_f$-TPPM. The new adaptation of $SW_f$-TPPM provides better decoupling characteristics for solid samples proved by experiments and simulations. The results are summarized below.

Fig. 1a and b shows the $^{13}C$ NMR spectrum of U-$^{13}C$-labeled tyrosine with its molecular structure acquired with supercycled $SW_f$-TPPM decoupling. A decoupling power of 90 kHz was applied here with a MAS frequency of 14 kHz. In general SPINAL-64 and $SW_f$-TPPM sequences perform well for all the $^{13}C$ resonances in the molecule. An enhancement in the intensities of all the peaks is observed when $SW_f$-TPPMS is applied as the decoupling sequence. For instance, Fig. 1c depicts the intensity comparison of the decoupled $^{13}C$ signal of $CH_2$ carbon of the molecule which is marked with an asterisk in the spectrum using SPINAL-64, $SW_f$-TPPM and $SW_f$-TPPMS decoupling sequences. All the decoupling sequences are at their optimized values. For $SW_f$-TPPM and $SW_f$-TPPMS, an optimized phase angle of 15° is used. In all cases, the proton offset frequency is kept at 7.75 kHz which is far from the on-resonance position of the selected $CH_2$ peak. A significant enhancement in the intensity, approximately 4%, is visible here for the $CH_2$ carbon and a similar improvement can be observed in all the other $^{13}C$ resonances.

Intensity gain for the decoupled resonances is one of the desirable features for a good decoupling scheme. But, the sequence should also be sturdy in performance with respect to various experimental parameters such as the offset of the RF irradiation, pulse phase angles and RF field strength. Experiments and numerical calculations were done towards understanding these aspects for the SPINAL-64, $SW_f$-TPPM and $SW_f$-TPPMS decoupling sequences and comparisons were made.

Fig. 2a depicts the intensities of the $CH_2$ (at 36 ppm) carbon in the decoupled $^{13}C$ spectra of tyrosine molecule acquired as a function of proton offset for SPINAL-64, $SW_f$-TPPM and $SW_f$-TPPMS decoupling. It may be observed from this figure that as the proton off-resonance value increases the efficiency of $SW_f$-TPPMS scheme remains mostly unaffected. For instance, the intensity gain for the $CH_2$ signal observed with $SW_f$-TPPMS decoupling scheme at a proton offset of 7.75 kHz is approximately 4% when compared to its parent version as seen in Fig. 2a. This point is further illustrated by presenting the intensities of the CH (130 ppm) carbon in the decoupled $^{13}C$ spectra of tyrosine molecule as a function of proton offset for SPINAL-64, $SW_f$-TPPM and $SW_f$-TPPMS decoupling in Fig. 2b. Again, as the proton off-resonance value increases the efficiency of decoupling using $SW_f$-TPPMS scheme remains relatively unaffected in comparison with SPINAL-64 and $SW_f$-TPPM. In other words, $SW_f$-TPPMS decoupling scheme functions more effectively when compared to SPINAL-64 and $SW_f$TPPM with respect to proton offset and hence gives more decoupling band width. When there is a necessity to cover large band width consistently, the relatively higher insensitivity of $SW_f$-TPPMS scheme is advantageous.

**Table 1**
Spectral intensity comparison of two selected $^{13}C$ resonances in the decoupled $^{13}C$ spectra of tyrosine at different decoupling powers of 90 kHz and 75 kHz using SPINAL-64, $SW_f$-TPPM and $SW_f$-TPPMS sequences. The MAS frequencies were 6, 8 and 14 kHz.

| Selected $^{13}C$ resonance and its peak position | RF field strength (kHz) | Decoupling sequence | Relative intensities at MAS frequencies of | | |
|---|---|---|---|---|---|
| | | | 6 kHz | 8 kHz | 14 kHz |
| $CH_2$ at 36 ppm | 90 | SPINAL-64 | 74 | 84 | 91 |
| | | $SW_f$-TPPM | 75 | 86 | 93 |
| | | $SW_f$-TPPMS | 75 | 87 | 94 |
| | 75 | SPINAL-64 | 66 | 80 | 81 |
| | | $SW_f$-TPPM | 67 | 81 | 82 |
| | | $SW_f$-TPPMS | 69 | 83 | 84 |
| CH at 130 ppm | 90 | SPINAL-64 | 37 | 68 | 98 |
| | | $SW_f$-TPPM | 37 | 68 | 98 |
| | | $SW_f$-TPPMS | 38 | 69 | 99 |
| | 75 | SPINAL-64 | 36 | 65 | 94 |
| | | $SW_f$-TPPM | 37 | 66 | 95 |
| | | $SW_f$-TPPMS | 37 | 68 | 95 |

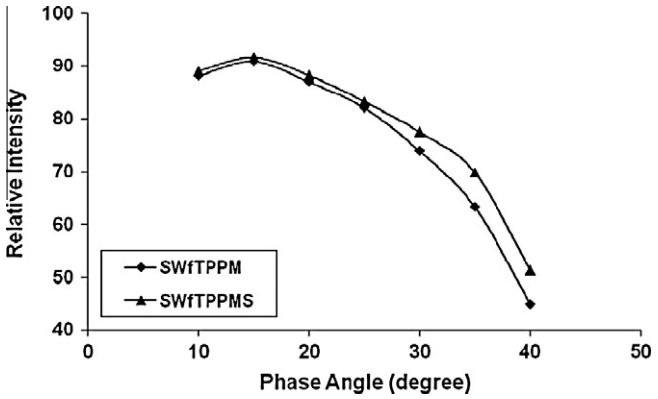


**Fig. 3.** The relative intensities of $CH_2$ peak (36 ppm) in the decoupled $^{13}C$ spectra of tyrosine at a decoupling power of 90 kHz as a function of phase angle $\varphi$ for $SW_f$-TPPM and $SW_f$-TPPMS decoupling sequences. The MAS frequency is kept at 14 kHz.

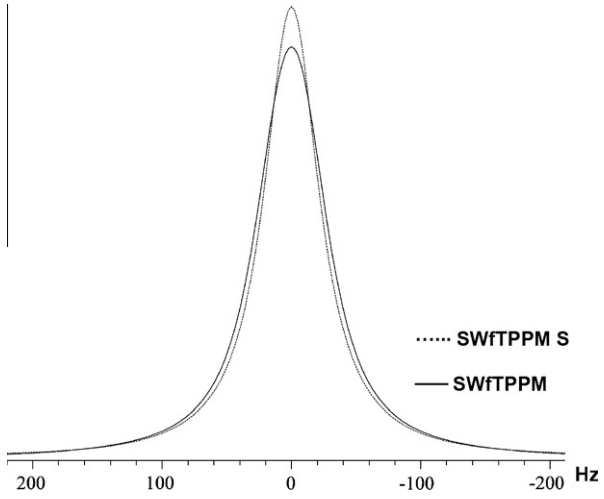


**Fig. 4.** Simulated $^{13}C$ NMR spectrum of a $CH_2$ system decoupled with $SW_f$-TPPM and its supercycled version. RF strength is 90 kHz with a MAS rate of 18 kHz. Phase angle is 20°.

Table 1 shows the spectral intensity comparison of the $CH_2$ peak (36 ppm) and CH peak (130 ppm) in the decoupled $^{13}C$ spectra of tyrosine at two different decoupling powers 90 and 75 kHz using SPINAL-64, $SW_f$-TPPM and $SW_f$-TPPMS sequences. The MAS frequencies were 6, 8 and 14 kHz. In each case the intensity is normalized with respect to the absolute intensity of the decoupled $^{13}C$ carbon of CH (130 ppm) recorded with $SW_f$-TPPMS using an RF power of 90 kHz at a proton offset of 3.75 kHz and a MAS frequency of 14 kHz which is the highest absolute intensity value among all the experiments. The performance of all the decoupling schemes is reasonable, but $SW_f$-TPPMS shows relatively higher intensity for the decoupled $^{13}C$ carbon of $CH_2$ at different MAS frequencies tested here as shown in the data (Table 1). For CH group, the efficiency of decoupling shown by SPINAL-64, $SW_f$-TPPM and $SW_f$-TPPMS sequences is comparable at different MAS frequencies and decoupling powers, because the homonuclear $^1H$–$^1H$ and heteronuclear $^1H$–$^{13}C$ dipolar couplings in tyrosine molecule are weaker in the case of CH group when compared with the $CH_2$ group. However, considering the overall spectral appearance and the data shown below it can be concluded that the $SW_f$-TPPMS shows its improved performance over the investigated range of MAS frequencies.

Fig. 3 shows the relative intensities of $CH_2$ peak (36 ppm) in the decoupled $^{13}C$ spectra of tyrosine at a decoupling power of 90 kHz as a function of phase angle $\varphi$ for $SW_f$-TPPM and $SW_f$-TPPMS decoupling sequences. The MAS frequency is kept at 14 kHz. Here, different experiments were done by varying phase angles from 10° to 40° with an increment of 5° and relative intensities of the decoupled $CH_2$ peak is analyzed with respect to phase angle, $\varphi$. It was observed that an optimum phase angle of 15° gives better decoupling for both $SW_f$-TPPM and $SW_f$-TPPMS. The efficiency of decoupling at larger phase angles deteriorates in both cases as shown in Fig. 3, but the supercycled sequence still shows considerable enhancement in the intensities of the decoupled peaks.

The efficiency of decoupling shown by $SW_f$-TPPMS was numerically analyzed and compared with its parent sequence in Figs. 4–6. Fig. 4 gives the simulated $^{13}C$ NMR spectrum of a $CH_2$ system decoupled with $SW_f$-TPPM and its supercycled version. A phase angle of 20° is used in the sequences and the RF field strength is 90 kHz with a MAS frequency of 18 kHz. In these simulations, homonuclear and heteronuclear dipolar interactions of the $CH_2$ spin system are included. It is observed that the supercycled version gives better decoupling and there is significant enhancement in the intensity of the peak corresponding to the $CH_2$ system as shown in the diagram. In Fig. 5, the relative intensities of the decoupled $^{13}C$ spectra of a $CH_2$ system is plotted as a function of MAS frequency and RF field strength for both $SW_f$-TPPMS and its parent sequence, $SW_f$-TPPM at a constant phase angle of 20°. A matrix of RF strength $\upsilon_1$ and MAS frequency was traced for each simulation. Also, $\upsilon_1$ is varied from 80 to 160 kHz with an increment of 10 kHz and MAS frequency is changed from 5 to 25 kHz with 5 kHz

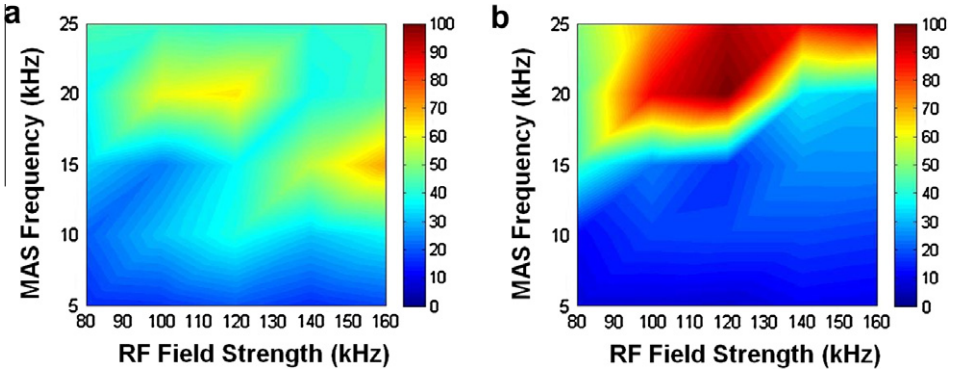


**Fig. 5.** The relative intensities of the decoupled $^{13}C$ spectra of a $CH_2$ system simulated for (a) $SW_f$-TPPM and (b) $SW_f$-TPPMS as a function of MAS frequency and RF field strength. Phase angle is kept at 20°. The RF field strength is changed from 80 to 160 kHz with an increment of 10 kHz and MAS frequency is varied from 5 to 25 kHz with 5 kHz increments.

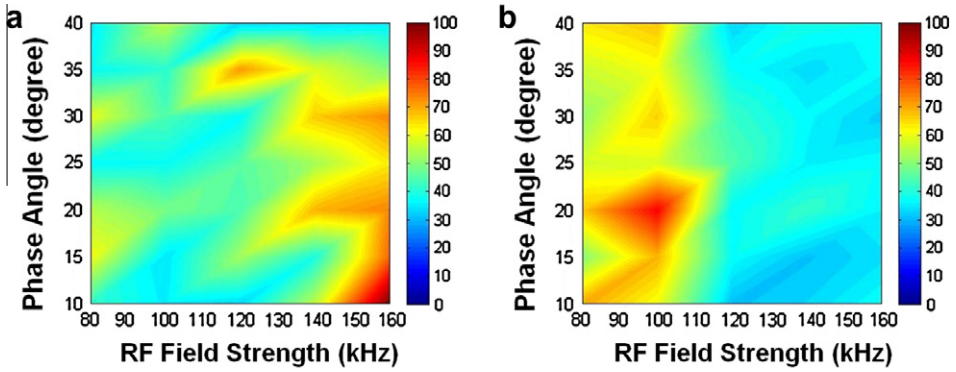


**Fig. 6.** The relative intensities of the decoupled $^{13}C$ spectra of a $CH_2$ system simulated for (a) $SW_f$-TPPM and (b) $SW_f$-TPPMS as a function of phase angle and RF field strength. The MAS frequency is 16 kHz. The RF field strength is varied from 80 to 160 kHz with an increment of 10 kHz and phase angle $\varphi$ is changed from 10° to 40° with 5° increments.

increments. The red[1] colored region in these contours represent efficient decoupling, and $SW_f$-TPPMS gives better performance uniformly over a larger range of parameters. For instance, in the low RF power region of 80–100 kHz, $SW_f$-TPPMS is better than its parent version at the MAS frequencies ranging from 15 to 25 kHz. Similarly, the relative intensities of the decoupled $^{13}C$ spectra of a $CH_2$ system is numerically analyzed for both $SW_f$-TPPMS and its parent sequence, $SW_f$-TPPM at a constant MAS frequency as a function of phase angle, $\varphi$ and RF field strength $\upsilon_1$ and plotted in Fig. 6. Here $\upsilon_1$ is varied from 80 to 160 kHz with an increment of 10 kHz and phase angle $\varphi$ is changed from 10° to 40° with 5° increments. A spread of good decoupling condition in the low power region is noticeable for $SW_f$-TPPMS when compared to its parent version.

## 4. Conclusions

The supercycled version of $SW_f$-TPPM, namely $SW_f$-TPPMS was investigated in solid samples for heteronuclear dipolar decoupling and its performance was compared with other commonly used decoupling schemes like SPINAL-64 and the parent $SW_f$-TPPM. From experiments performed in a standard sample of U-$^{13}C$-labeled tyrosine, it was found that besides providing intensity gain for all the $^{13}C$ resonances of the sample, the $SW_f$-TPPMS shows good decoupling characteristics with respect to proton offset and MAS frequencies. The performance of $SW_f$-TPPMS remains relatively unaffected within the investigated range of the decoupler offset frequency. Within the range of MAS frequencies analyzed, $SW_f$-TPPMS performs better than the other schemes. Also, this decoupling scheme is user-friendly, simple and easy to formulate and optimize for usual application on modern NMR spectrometers. It is advisable to use this supercycled sequence $SW_f$-TPPMS for heteronuclear dipolar decoupling which can give effective performance in solid-state NMR.

## Acknowledgments

The authors would like to thank Professor K.V. Ramanathan for giving us a chance to perform these experiments at the NMR Research Center of Indian Institute of Science, Bangalore. The help provided by Dr. S. Jayanthi in carrying out the experiments is greatly appreciated. We thank Dr. P.K. Madhu for a careful reading of the manuscript. The financial support for Cyril Augustine comes from the University Grants Commission (UGC), India.

[1] For interpretation of color in Figs. 5 and 6, the reader is referred to the web version of this article.

## References

[1] P. Hodgkinson, Heteronuclear decoupling in the NMR of solids, Prog. Nucl. Magn. Reson. Spectrosc. 46 (2005) 197–222.
[2] M. Ernst, Heteronuclear spin decoupling in solid-state NMR under magic-angle sample spinning, J. Magn. Reson. 162 (2003) 1–34.
[3] A.E. Bennett, C.M. Rienstra, M. Auger, K.V. Lakshmi, R.G. Griffin, Heteronuclear decoupling in rotating solids, J. Chem. Phys. 103 (1995) 6951–6958.
[4] M.H. Levitt, R. Freeman, T. Frenkiel, Supercycles for broadband heteronuclear decoupling, J. Magn. Reson. 50 (1982) 57–160.
[5] A.J. Shaka, J. Keeler, Broadband spin decoupling in isotropic liquids, Prog. NMR Spectrosc. 19 (1987) 47–129.
[6] Y. Yu, B.M. Fung, An efficient broadband decoupling sequence for liquid crystals, J. Magn. Reson. 130 (1998) 317–320.
[7] B.M. Fung, A.K. Khitrin, K. Ermolaev, An improved broadband decoupling for liquid crystals and solids, J. Magn. Reson. 142 (2000) 97–101.
[8] G. De Paëpe, D. Sakellariou, P. Hodgkinson, S. Hediger, L. Emsley, Heteronuclear decoupling in NMR of liquid crystals using continuous phase modulation, Chem. Phys. Lett. 368 (2003) 511–522.
[9] A. Detken, E.H. Hardy, M. Ernst, B.H. Meier, Simple and efficient decoupling in magic-angle spinning solid-state NMR: the XiX scheme, Chem. Phys. Lett. 356 (2002) 298–304.
[10] M. Eden, M.H. Levitt, Pulse sequence symmetries in the nuclear magnetic resonance of spinning solids: application to heteronuclear decoupling, J. Chem. Phys. 111 (1999) 1511–1519.
[11] J. Leppert, O. Ohlenschläger, M. Görlach, R. Ramachandran, Adiabatic heteronuclear decoupling in rotating solids, J. Biomol. NMR 29 (2004) 319–324.
[12] G.D. Paëpe, B. Eléna, L. Emsley, Characterization of heteronuclear decoupling through proton spin dynamics in solid-state nuclear magnetic resonance spectroscopy, J. Chem. Phys. 121 (2004) 3165–3180.
[13] X. Filip, C. Tripon, C. Filip, Heteronuclear decoupling under fast MAS by a rotor-synchronized Hahn-echo pulse train, J. Magn. Reson. 176 (2005) 239–243.
[14] R.S. Thakur, N.D. Kurur, P.K. Madhu, Swept-frequency two-pulse phase modulation for heteronuclear dipolar decoupling in solid-state NMR, Chem. Phys. Lett. 426 (2006) 459–463.
[15] R.S. Thakur, N.D. Kurur, P.K. Madhu, Improved heteronuclear dipolar decoupling sequences for liquid-crystal NMR, J. Magn. Reson. 185 (2007) 264–269.
[16] R.S. Thakur, N.D. Kurur, P.K. Madhu, An analysis of phase modulated heteronuclear dipolar decoupling sequences in solid-state nuclear magnetic resonance, J. Magn. Reson. 193 (2008) 77–88.
[17] R.S. Thakur, N.D. Kurur, P.K. Madhu, An experimental study of decoupling sequences for multiple-quantum and high-resolution MAS experiments in solid-state NMR, Magn. Reson. Chem. 46 (2008) 166–169.
[18] C.V. Chandran, P.K. Madhu, N.D. Kurur, T. Bräuniger, Swept-frequency two-pulse phase modulation ($SW_f$-TPPM) sequences with linear sweep profile for heteronuclear decoupling in solid-state NMR, Magn. Reson. Chem. 46 (2008) 943–947.
[19] C.V. Chandran, T. Bräuniger, Efficient heteronuclear dipolar decoupling in solid-state NMR using frequency-swept SPINAL sequences, J. Magn. Reson. 200 (2009) 226–232.
[20] C.V. Chandran, P.K. Madhu, P. Wormald, T. Bräuniger, Frequency-swept pulse sequences for $^{19}F$ heteronuclear spin decoupling in solid-state NMR, J. Magn. Reson. 206 (2010) 255–263.
[21] C. Augustine, N.D. Kurur, Heteronuclear dipolar decoupling in liquid-crystal NMR using supercycled $SW_f$-TPPM sequences, Magn. Reson. Chem. 48 (2010) 798–803.
[22] R. Fu, Efficient heteronuclear dipolar decoupling in NMR of static solid samples using phase-wiggled two-pulse phase modulation, Chem. Phys. Lett. 483 (2009) 147–153.
[23] M. Bak, J.T. Rasmussen, N.C. Nielsen, SIMPSON: a general simulation program for solid-state NMR Spectroscopy, J. Magn. Reson. 147 (2000) 296–330.